Desalination and Water Treatment
www.deswater.com
doi: 10.1080/19443994.2014.989273

57 (2016) 3975–3984
February

Taylor & Francis
Taylor & Francis Group

Magnetic hydroxypropyl chitosan functionalized graphene oxide as adsorbent for the removal of lead ions from aqueous solution

Yaoguang Wang, Tao Yan, Liang Gao, Limei Cui, Lihua Hu, Liangguo Yan, Bin Du*, Qin Wei

Key Laboratory of Chemical Sensing & Analysis in Universities of Shandong, School of Chemistry and Chemical Engineering, University of Jinan, Jinan 250022, China, Tel. +86 531 82767872; emails: wang_yao_guang@163.com (Y. Wang), chm_yant@ujn.edu.cn (T. Yan), jndxgaoliang@126.com (L. Gao), clm030124@163.com (L. Cui), Tel. +86 531 82760510; email: lianlianfengchen04@163.com (L. Hu), Tel. +86 531 82767872; email: yanyu_33@163.com (L. Yan), Tel./Fax: +86 531 82767370; email: dubin61@gmail.com (B. Du), Tel. +86 531 82765730; email: sdjndxwq@163.com (Q. Wei)

Received 30 April 2014; Accepted 12 November 2014

ABSTRACT

Magnetic hydroxypropyl chitosan/graphene oxide (MHCGO) composites have been synthesized and employed as adsorbent for removal of lead ions from aqueous solution. X-ray powder diffraction, Fourier transform infrared spectrum, and scanning electron microscope showed that the MHCGO composites were fabricated successfully. The effects of adsorbent dosage, pH, and contact time on the adsorption of lead ions have been discussed, and the optimal adsorption conditions have been acquired. The results indicated that the adsorption of lead ions on MHCGO was dependent on pH with the optimum pH nearly 5.5. The adsorption process was fairly quick and the time to reach adsorption equilibrium is 100 min. The adsorption kinetics could be described by the pseudo-second-order model very well. Adsorption data fitted well with Freundlich model. The effect of temperature on lead ions adsorption was studied and was shown to be spontaneous.

Keywords: Adsorption; Hydroxypropyl chitosan; Graphene oxide; Lead ions

1. Introduction

Lead ions are common toxic non-biodegradable pollutants, which can accumulate in human skeleton, brain, kidney and muscles, leading to fatigue, irritability, anemia, mental retardation, kidney damage, and other diseases [1,2]. With the development of chemical industry more and more wastewater containing lead ions are discharged and affects the health of creatures greatly [3,4]. Therefore, a lot of researchers throughout the world are working at solving this issue [5,6].

Various techniques have been applied to remove lead ions from wastewater, such as chemical precipitation, membrane processes, ion exchange, flocculation, reverse osmosis, and adsorption [7–11]. Among them, adsorption has been one of the most commonly used techniques because of its simple operation and wide application scope. However, the conventional adsorbents have disadvantages such as low adsorption efficiency, small capacity, and poor selectivity. Therefore, it is important to develop new low-cost and efficient adsorbents in order to improve adsorption [12].

*Corresponding author.

In recent years, large numbers of adsorbents, such as zeolites, clays, metal oxides, and activated carbons were investigated [13–16], among which graphene oxide (GO) has been a hot spot. Because of its unique two-dimensional structure and large specific surface area, it is an ideal material to adsorb metal ions [17–20]. Chitosan also showed favorable adsorption properties for the adsorption of metal ions [21–23]. Recently, the application of chitosan/graphene oxide composites as adsorbents has been proved to be probable [24]. However, hardly has anyone used the derivatives of chitosan linked with GO as adsorbents for the adsorption of metal ions. In terms of the separation of adsorbent and adsorbate, addition of magnetic material can achieve rapid separation of adsorbent from solution. Based on these facts, we proposed a new kind of adsorbent of magnetic hydroxypropyl chitosan/graphene oxide (MHCGO) composites. The adsorbent could be easily synthesized and applied to remove lead ions from aqueous solution. The separation from water of the magnetic adsorbent was easily and readily achieved by a magnet once the adsorption process completed. The application of MHCGO composites for removal of lead ions with the help of external magnetic field is shown in Scheme 1. And the prepared adsorbent may provide potential application in solving the issue of wastewater treatment.

2. Experimental

2.1. Apparatus and reagents

Hydroxypropyl chitosan was purchased from Nantong Lushen Bioengineering Co., Ltd. (China). Glutaraldehyde was purchased from Tianjin Kemiou Chemical Reagent Co., Ltd. (China). Magnetic $SrFe_{12}O_{19}$ was obtained from Nanjing Emperor Nano Material Co., Ltd. All other chemicals were of analytical reagents grade and double-distilled water was used in the preparation of all solutions.

Scanning electron microscope (SEM) images were obtained using field emission SEM (Hitachi S-4800). Fourier transform infrared (FTIR) spectra of samples were recorded with KBr pellet in the range of 4,000–400 cm^{-1} on Perkin-Elmer 580B spectrophotometer (Perkin-Elmer Inc., America). Wide angle X-ray diffraction (WAXRD) patterns were recorded by a D8 ADVANCE X-ray diffraction spectrometer (Bruker, German) with a Cu Kα target at a scan rate of 0.03° 2θ s^{-1} from 5° to 80°.

2.2. Preparation of GO

GO powder was synthesized from graphite by using a modified Hummer's method [25,26]. In a typical method, 0.5 g of graphite was oxidized by 10 mL of concentrated H_2SO_4 under stirring for 12 h. Then,

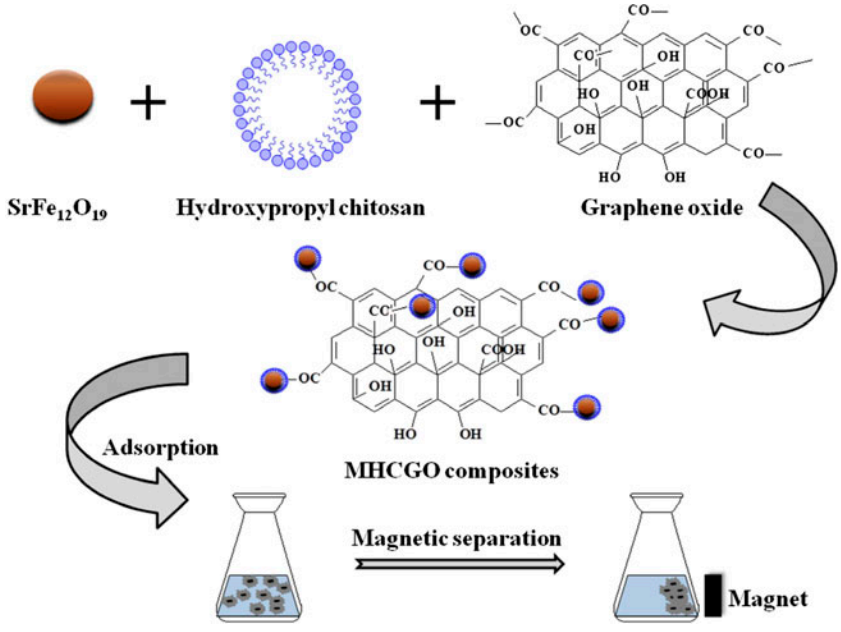

Scheme 1. The application of MHCGO composites for removal of lead ions with the help of external magnetic field.

3.0 g of $KMnO_4$ was added slowly at 0℃. After the addition of $KMnO_4$, the solution was stirred at 100℃ for another 12 h to fully oxidize graphite. The GO was then washed and dried.

2.3. Preparation of MHCGO composites

The preparation procedure of MHCGO composites was as follows: Firstly, 0.4 g of hydroxypropyl chitosan was dissolved into the mixture of H_2O (20 mL) and glacial acetic acid (5 mL) in a three-neck flask, then the mixture was dispersed under ultrasonic about 2 h at room temperature. Secondly, 0.1 g of magnetic $SrFe_{12}O_{19}$ was added into the above-mixed solution and the reaction was operated under mechanical stirring for 1.5 h, then 3 mL of liquid paraffin was injected slowly under stirring. After 0.5 h of reaction, 3 mL of glutaraldehyde was added. At last, 0.1 g of GO was added and the mixture was stirred continuously for 90 min at 50℃ in oil bath. The pH of the mixture was controlled between 9.0 and 10.0 by 2.0 mol L^{-1}NaOH, and the mixture was kept in oil bath for another 60 min at 80℃. The obtained products were washed by petroleum ether, ethanol, and distilled water until the pH was about 7.0.

2.4. Batch adsorption experiment

All batch adsorption experiments were operated on a SHZ-82A water bath oscillator. Twelve milligram of MHCGO and 25 mL of the solution containing lead ions were added into 100 mL beaker flask and then shaken in water bath at room temperature. After a

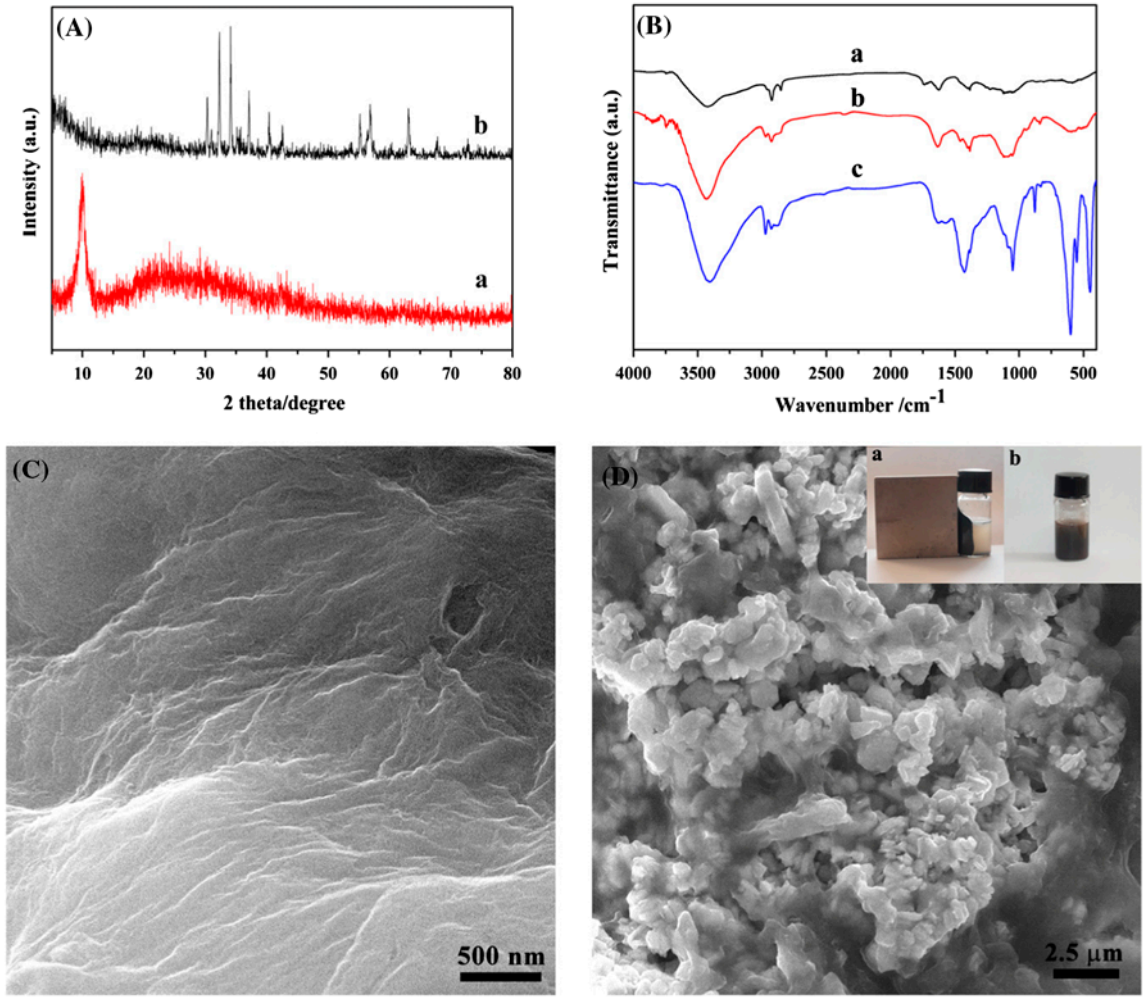

Fig. 1. (A) XRD patterns of GO (a) and MHCGO composites (b); (B) FTIR spectrum of GO (a), hydroxypropyl chitosan (b) and MHCGO composites (c); (C) SEM image of GO; and (D) SEM image of MHCGO composites, the insets are the presence of external magnetic field (a) and the absence of additional magnetic field (b).

certain time, the beaker flask was taken out and the magnet was used for the separation of magnetic adsorbent from the solution.

The adsorbent dosage was measured ranging from 2 to 20 mg for 25 mL of 40 mg L^{-1} lead ions solution. The effect of pH on the adsorption process was evaluated in the pH range of 2.0–6.5 for 180 min. The adsorption kinetics was studied by investigating the adsorption after different contact time from 3 to 300 min. To obtain the adsorption isotherms, solutions with different initial concentrations were disposed as same as the above. The residual lead ions were measured using a UV–Vis spectrophotometer (Perkin-Elmer Lambda 35). The adsorption capacity and the adsorption rate were calculated according to the equations as follows:

$$Q = \frac{C_0 - C_e}{m} \times V \quad (1)$$

$$X = \frac{C_0 - C_e}{C_0} \times 100\% \quad (2)$$

where C_0 and C_e are the initial concentration and the equilibrium concentration of lead ions, respectively (mg L^{-1}); Q is the adsorption amount (mg g^{-1}); X is the adsorption efficiency; m is the amount of adsorbent (g); V is the volume of lead ions solution (L).

3. Results and discussion

3.1. Characterizations of MHCGO composites

The X-ray powder diffraction (XRD) patterns of the as-synthesized MHCGO composites (Fig. 1(A)) were obtained and analyzed. The peaks at $2\theta = 30.33^\circ$ (110), 32.35° (107), 34.18° (114), 37.12° (203), 40.38° (205), and 63.13° (220) are indicative of magnetic $SrFe_{12}O_{19}$ in MHCGO composites. It is in good agreement with the standard profile JCPDS 33-1340. Compared with the pure GO-diffracted signals, there are no signals of GO in MHCGO composites at 10°, which may be ascribed to the following two reasons: (1) the magnetic $SrFe_{12}O_{19}$ particles reduce the aggregation of GO, which results in more fewer layered GO and weaker peaks from carbon; (2) the strong signals of the magnetic $SrFe_{12}O_{19}$ particles tend to overlap the carbon peaks.

Fig. 1(B) shows the FTIR spectra of GO (a), hydroxypropyl chitosan (b), and MHCGO composites (c). In the spectrum of GO, the peaks at 3,430, 1,746, 1,621, 1,400, 1,228, and 1,114 cm^{-1} are attributed to the O–H, C=O in –COOH, aromatic C=C, carboxyl C–O, epoxy C–O, and alkoxyl C–O stretches, respectively [27–29]. As shown in Fig. 1(B), (b), the absorption peak at around 3,427 cm^{-1} indicates the stretching vibration of N–H group bonded with O–H group in hydroxypropyl chitosan, and at 1,633 cm^{-1} demonstrates N–H bending vibration. Compared to GO and hydroxypropyl chitosan, the FTIR spectrum of MHCGO composites not only contains the aforementioned absorption peaks, but also shows new absorption peaks at 451 and 606 cm^{-1}, which are the characteristic peaks of $SrFe_{12}O_{19}$, and the results indicate that the magnetic $SrFe_{12}O_{19}$ particles were connected with GO and hydroxypropyl chitosan successfully.

Fig. 1(C) and (D) display the SEM images of GO and MHCGO composites, respectively. In Fig. 1(C), it is clear that the paper-like GO are thin layered, which is beneficial for the loading of magnetic $SrFe_{12}O_{19}$ particles. The image of MHCGO composites (shown in Fig. 1(D)) indicates that GO are tightly bound onto the $SrFe_{12}O_{19}$ particles. The observed rough surface of $SrFe_{12}O_{19}$ particles and the pores among the particles may improve the adsorption of the MHCGO composites. Furthermore, the insets in Fig. 1(D) are of the sample, in the presence (a) and in the absence (b) of external magnetic field, demonstrating the magnetic separation effect of MHCGO composites, as the result of the existence of $SrFe_{12}O_{19}$ particles.

3.2. Effect of adsorbent dosage on the adsorption of lead ions

The effect of the adsorbent mass on lead ions adsorption was studied in order to choose the optimal adsorbent dosage. The experiment was carried out in 25 mL of lead ions solution at 25℃ with the dosage of adsorbent ranging from 2 to 20 mg. As can be seen in Fig. 2(A), with the increase in adsorbent dosage, the adsorption efficiency increases rapidly. Then, the adsorption efficiency increases slowly when the adsorbent dosage reaches 12 mg. Finally, the change of adsorption efficiency is not obvious. Considering the removal efficiency and practicality, 12 mg of the adsorbent was selected as the optimal dosage for the succeeding studies.

3.3. Effect of pH on the adsorption of lead ions

The pH of the solution has been regarded as an important factor on the adsorption of metal ions [30]. Therefore, the effect of pH ranging from 2.0 to 6.5 on the adsorption was investigated, and the results are shown in Fig. 2(B). When the solution was at low pH, the adsorption efficiency was low and increased slowly. As the pH increased, the adsorption efficiency increased rapidly, and the maximum adsorption

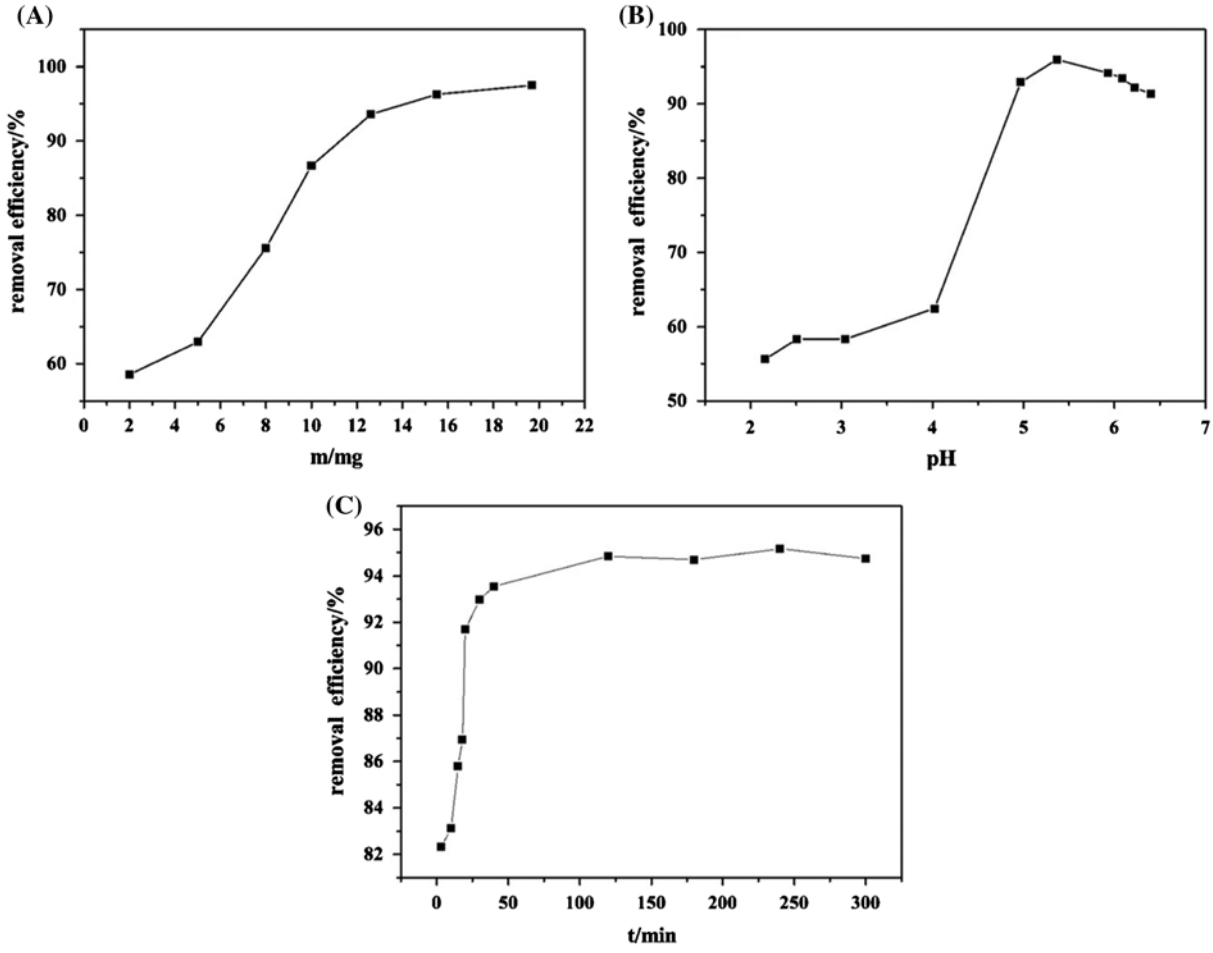

Fig. 2. Effects of adsorbent dosage (A), pH (B), and contact time (C) on the adsorption of lead ions.

efficiency was arrived at a pH of nearly 5.5. The poor adsorption efficiency at low pH can be interpreted as, hydrogen ions and lead ions being competitively adsorbed on the surface sites at low pH [31]. The amino groups on the surface of MHCGO composites can be easily protonated to be $–NH_3^+$ leading to only a small amount of $–NH_2$ combining with Pb^{2+}. In addition, the electrostatic repulsion between $–NH_3^+$ and Pb^{2+} further reduces the adsorption of lead ions onto the composites. With the increase in pH, the protonated $–NH_3^+$ decreases. More $–NH_2$ recover and the adsorption amount of Pb^{2+} increase. Then, at higher pH, OH^- can be adsorbed onto the surface of $–NH_2$ competing with Pb^{2+}, leading to a reduction in the amount of adsorbed Pb^{2+}. The adsorption is obviously a chemisorption process and can be expressed by following reactions:

$$–NH_2 + H^+ = –NH_3^+, –NH_2 + Pb^{2+} = –NH_2Pb^{2+}$$

$$–NH_2 + OH^- = –NH_2OH^-, –NH_2OH^- + Pb^{2+} = –NH_2OH^- \cdots Pb^{2+}$$

Therefore, pH of 5.5 was chosen as the optimal pH for Pb^{2+} solution in the succeeding adsorption experiment.

3.4. Effect of contact time on the adsorption of lead ions and adsorption kinetics

The effect of contact time for the MHCGO composites on the adsorption of lead ions is shown in Fig. 2(C). The adsorbent displayed excellent adsorption capacity in the first 60 min. And the adsorption equilibrium time was about 100 min. After 120 min, the adsorption capacity had no obvious change. Therefore, the optimal contact time for the adsorption of lead ions is considered to be 120 min.

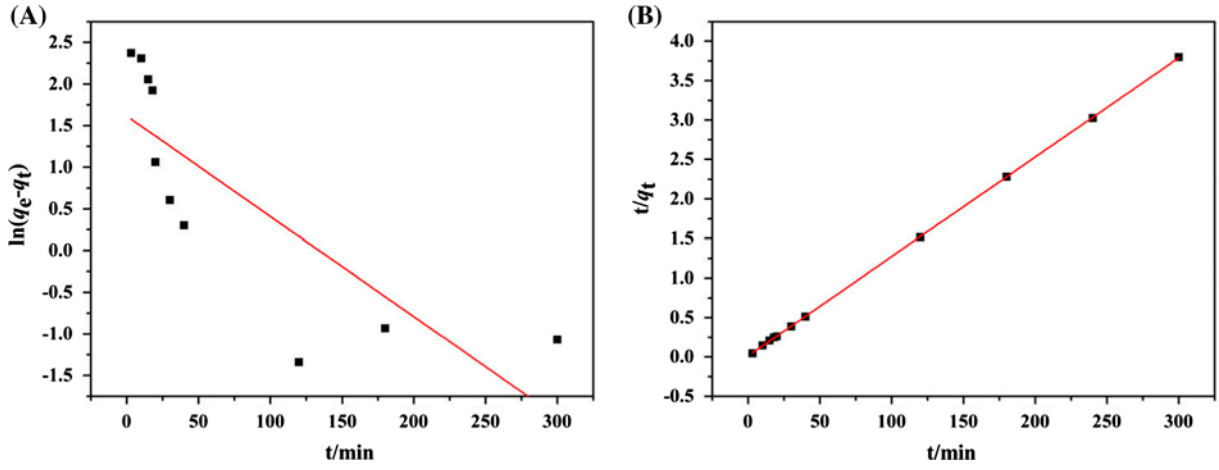

Fig. 3. Pseudo-first-order kinetic model (A) and pseudo-second-order kinetic model (B) for adsorption of lead ions.

The adsorption kinetics for the adsorption of lead ions was studied. And, the obtained adsorption data for lead ions were analyzed according to kinetic models expressed as follows:

Pseudo-first-order kinetic model [32]:

$$\ln(q_e - q_t) = \ln q_e - k_1 t \tag{3}$$

Pseudo-second-order kinetic model [33]:

$$\frac{t}{q_t} = \frac{1}{k_2 q_e^2} + \frac{t}{q_e} \tag{4}$$

where q_e (mg g^{-1}) is the amount of solute adsorbed at equilibrium, q_t (mg g^{-1}) is the amount of solute adsorbed at time t, k_1 (min^{-1}) is the pseudo-first-order rate constant, and k_2 (g mg^{-1} min^{-1}) is the rate constant for the pseudo-second-order equation.

Fig. 3 displays the fitting results of pseudo-first-order kinetic model and pseudo-second-order kinetic model. Observed from the two figures, it is clear that the adsorption data fit the pseudo-second-order kinetic model very well. The linear correlation coefficient of the pseudo-second-order kinetic model (R^2 = 0.9999) is higher than that of the pseudo-first-order kinetic model (R^2 = 0.6165). The results indicate that the adsorption may be controlled by the rate process. And the calculated adsorption capacity (79.43 mg g^{-1}) fits well with the experimental data (79.30 mg g^{-1}).

3.5. Adsorption isotherms

Four isotherm models have been applied to study the adsorption behavior between the solution and the adsorbent, namely, Langmuir, Henry, Temkin, and Freundlich [34,35]. The equations are expressed as follows:

Langmuir:

$$q_e = \frac{bq_m C_e}{1 + bC_e}, \text{ the linear form: } \frac{1}{q_e} = \frac{1}{q_m bC_e} + \frac{1}{q_m} \tag{5}$$

$$\text{Henry: } q_e = kc_e \tag{6}$$

$$\text{Temkin: } q_e = \frac{RT}{b_T}\ln c_e + \frac{RT}{b_T}\ln A_T \tag{7}$$

$$\text{Freundlich: } q_e = K_F c_e^{1/n}, \text{ the linear form: } \ln q_e = \ln K_F + \frac{1}{n}\ln c_e \tag{8}$$

The adsorption isotherms fitted by four models are shown in Fig. 4. The parameters calculated from the four models are listed in Table 1. As can be seen in Table 1, the adsorption process can be best described by Freundlich model (R^2 = 0.9694). The Freundlich isotherm model shows that the ratio of solute adsorbed on solid surface to the solute concentration is a function of the solution concentration. This model allows for several kinds of sorption sites on the solid and represents properly the sorption data at low concentrations and intermediate concentrations on heterogeneous surfaces [36,37]. The large value of K_f demonstrates that the adsorbent has a large adsorption capacity toward metal ions. And the value of n represents that the adsorption process takes place on the heterogeneous surfaces.

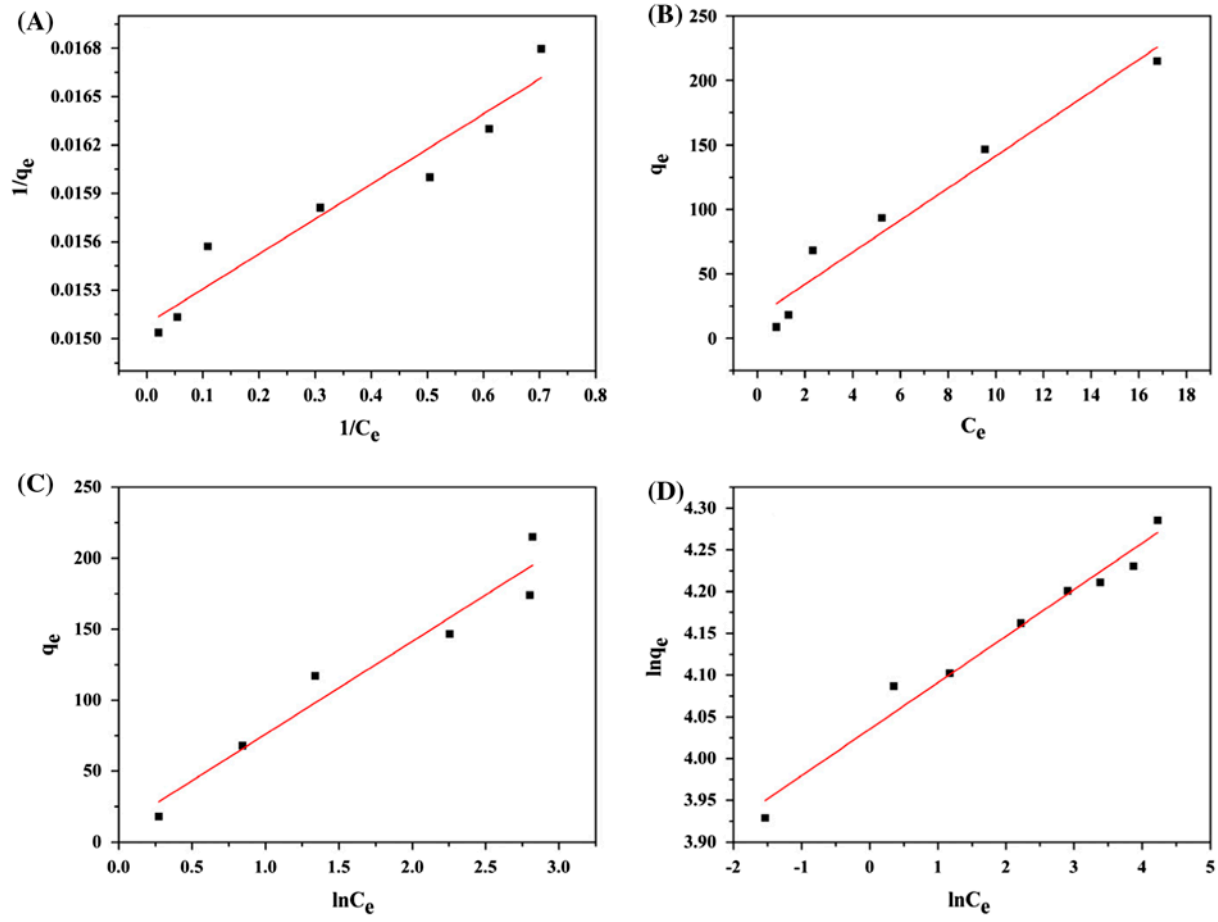

Fig. 4. Langmuir (A), Henry (B), Temkin (C), and Freundlich (D) isotherm for lead ions adsorption.

Table 1
The parameters for Langmuir, Henry, Temkin, and Freundlich isotherms

Models	Parameters	
Langmuir	q_m (mg g^{-1})	66.27
	b (L mg^{-1})	6.954
	R^2	0.9201
Henry	K_h	0.7092
	R^2	0.5642
Temkin	b_T	37.86
	A_T	1.174
	R^2	0.9322
Freundlich	K_f	56.56
	N	17.95
	R^2	0.9694

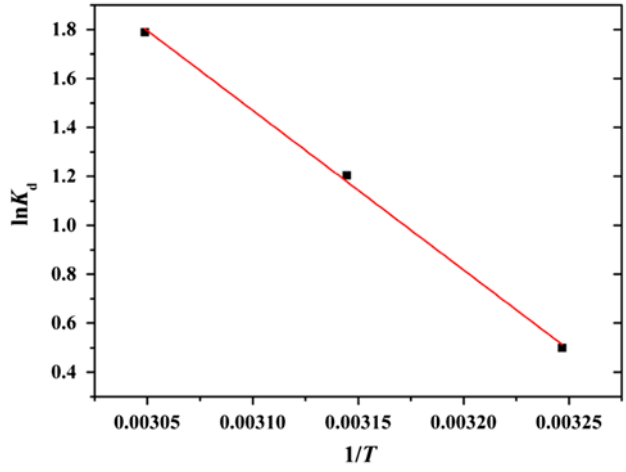

Fig. 5. Adsorption thermodynamic of lead ions adsorption onto MHCGO composites.

3.6. Adsorption thermodynamic

The effect of temperature of lead ions adsorption was studied at the temperatures of 308, 318, and 328 K. The changes of Gibbs free energies (ΔG), enthalpy (ΔH), and entropy (ΔS) can be calculated by the following equations:

Table 2
Thermodynamic parameters of lead ions adsorption at different temperatures

T (K)	ΔG (kJ mol^{-1})	ΔH (kJ mol^{-1})	ΔS (J mol^{-1} K^{-1})
308	−1.280	54.21	180.3
318	−3.185		
328	−4.881		

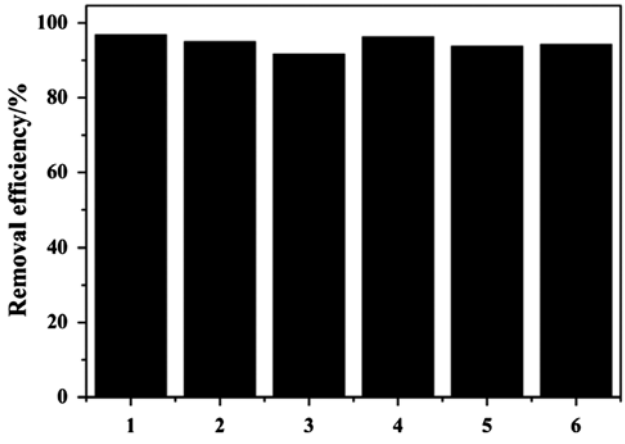

Fig. 6. The effect of coexisting ions in lead ions solution (1. None; 2. K^+; 3. Ca^{2+}; 4. Na^+; 5. Mg^{2+}; 6. $K^+ + Ca^{2+} + Na^+ + Mg^{2+}$).

$$\Delta G = -RT \ln K_d \quad (9)$$

$$\ln K_d = \frac{\Delta S}{R} - \frac{\Delta H}{RT} \quad (10)$$

where R is the universal gas constant (8.314 J mol^{-1} K^{-1}), T is the absolute temperature (in Kelvin), and K_d is the thermodynamic equilibrium constant. The results are shown in Fig. 5 and the thermodynamic parameters are listed in Table 2.

The positive value of ΔH indicates that the sorption of lead ions is an endothermic process, which is in accord with the principles of chemical adsorption. The values of ΔG become more negative from –1.280 to −4.881 kJ mol^{-1} with increase in temperature from 308 to 328 K, indicating more efficient adsorption on the solid surface, which may be due to the fact that lead ions are readily desolvated and hence, their sorption becomes more favorable. The positive value of the entropy changes (ΔS) indicates that the adsorption process was spontaneous [38].

Table 3
Comparison of adsorption capacities of various adsorbents for lead ions.

Adsorbents	q_m (mg g^{-1})	Ref.
MHCGO composites	79.30	This paper
Chitosan/magnetite	63.33	[39]
Chitosan/cellulose	26.31	[40]
Chitosan/sand	12.32	[41]
Mesoporous silica SBA-15	42.55	[42]
Bentonite	19.19	[43]
Waste mud	24.4	[44]
Montmorillonite	31.05	[45]
Natural zeolite	20.70	[46]
Fly ash	40.00	[47]
Palygorskite	20.72	[48]

3.7. Competing ions interference experiment

Both natural water and industrial wastewater contain different kinds of ions like K^+, Ca^{2+}, Na^+, and Mg^{2+}. In the adsorption process, the existence of these metal ions may affect the removal efficiency of lead ions. Therefore, the interference of these four metal ions for lead ions adsorption was also investigated. Solutions containing K^+, Ca^{2+}, Na^+, and Mg^{2+} were prepared by adding potassium nitrate, calcium nitrate, sodium nitrate, and magnesium nitrate into lead ions solution, respectively. The results are displayed in Fig. 6. And the relative standard deviation is 1.989% which demonstrates that the coexisting K^+, Ca^{2+}, Na^+, and Mg^{2+} have no distinct effect for lead ions adsorption.

3.8. Performance evaluations

A comparison of the maximum adsorption capacities (q_m) of MHCGO composites with the literature reports for lead ions adsorption is listed in Table 3. It can be seen that the maximum adsorption capacity of MHCGO composites is higher than that of other materials', which might be ascribed to the complexation capacity of MHCGO. It is obvious that some multiple magnetic composites perform better than single-component materials. Further researches associated with magnetic adsorbent are likely to carry out in the future to obtain better performance of adsorption.

4. Conclusions

In summary, the MHCGO composites were fabricated and applied to high efficient adsorption for lead ions in aqueous solution. The experimental results

showed that the adsorption process was strongly dependent on pH and the composites had a high adsorption capacity (79.30 mg g^{-1}). The adsorption data fitted Freundlich model better than Langmuir, Henry, and Temkin models. The adsorption kinetics of lead ions on MHCGO composites could be well described by pseudo-second-order model. The adsorption thermodynamic results indicated that the adsorption process was spontaneous. Therefore, the combination of the magnetic substances with the superior adsorption properties of GO and hydroxypropyl chitosan could make a powerful separation material to deal with the removal of metal ions in natural environment.

Acknowledgements

This study was supported by the Natural Science Foundation of China (No. 21175057, 21375047, 21377046), the Science and Technology Plan Project of Jinan (No. 201307010), and QW thanks the Special Foundation for Taishan Scholar Professorship of Shandong Province and UJN (No. ts20130937).

References

[1] T. Sheela, Y.A. Nayaka, Kinetics and thermodynamics of cadmium and lead ions adsorption on NiO nanoparticles, Chem. Eng. J. 191 (2012) 123–131.
[2] V. Inglezakis, M. Loizidou, H. Grigoropoulou, Equilibrium and kinetic ion exchange studies of Pb^{2+}, Cr^{3+}, Fe^{3+} and Cu^{2+} on natural clinoptilolite, Water Res. 36 (2002) 2784–2792.
[3] Y. Al-Degs, M. Khraisheh, M. Tutunji, Sorption of lead ions on diatomite and manganese oxides modified diatomite, Water Res. 35 (2001) 3724–3728.
[4] S. Abdel-Halim, A. Shehata, M. El-Shahat, Removal of lead ions from industrial waste water by different types of natural materials, Water Res. 37 (2003) 1678–1683.
[5] S. Tunali, T. Akar, A.S. Özcan, I. Kiran, A. Özcan, Equilibrium and kinetics of biosorption of lead (II) from aqueous solutions by *Cephalosporium aphidicola*, Sep. Purif. Technol. 47 (2006) 105–112.
[6] M. Sekar, V. Sakthi, S. Rengaraj, Kinetics and equilibrium adsorption study of lead (II) onto activated carbon prepared from coconut shell, J. Colloid Interface Sci. 279 (2004) 307–313.
[7] M. Ghaedi, A. Shokrollahi, K. Niknam, E. Niknam, A. Najibi, M. Soylak, Cloud point extraction and flame atomic absorption spectrometric determination of cadmium (II), lead (II), palladium (II) and silver (I) in environmental samples, J. Hazard. Mater. 168 (2009) 1022–1027.
[8] O.D. Uluozlu, M. Tuzen, D. Mendil, M. Soylak, Coprecipitation of trace elements with Ni^{2+}/2-Nitroso-1-naphthol-4-sulfonic acid and their determination by flame atomic absorption spectrometry, J. Hazard. Mater. 176 (2010) 1032–1037.
[9] A. Karbassi, S. Nadjafpour, Flocculation of dissolved Pb, Cu, Zn and Mn during estuarine mixing of river water with the Caspian Sea, Environ. Pollut. 93 (1996) 257–260.
[10] M. Soylak, Y.E. Unsal, N. Kizil, A. Aydin, Utilization of membrane filtration for preconcentration and determination of Cu(II) and Pb(II) in food, water and geological samples by atomic absorption spectrometry, Food Chem. Toxicol. 48 (2010) 517–521.
[11] V.K. Gupta, I. Ali, Removal of lead and chromium from wastewater using bagasse fly ash—A sugar industry waste, J. Colloid Interface Sci. 271 (2004) 321–328.
[12] G.P. Rao, C. Lu, F. Su, Sorption of divalent metal ions from aqueous solution by carbon nanotubes: A review, Sep. Purif. Technol. 58 (2007) 224–231.
[13] E. Erdem, N. Karapinar, R. Donat, The removal of heavy metal cations by natural zeolites, J. Colloid Interface Sci. 280 (2004) 309–314.
[14] D. Kinniburgh, M. Jackson, J. Syers, Adsorption of alkaline earth, transition, and heavy metal cations by hydrous oxide gels of iron and aluminum, Soil Sci. Soc. Am. J. 40 (1976) 796–799.
[15] M. Kobya, E. Demirbas, E. Senturk, M. Ince, Adsorption of heavy metal ions from aqueous solutions by activated carbon prepared from apricot stone, Bioresour. Technol. 96 (2005) 1518–1521.
[16] D. Mohan, K.P. Singh, Single and multi-component adsorption of cadmium and zinc using activated carbon derived from bagasse—An agricultural waste, Water Res. 36 (2002) 2304–2318.
[17] L. Hao, H. Song, L. Zhang, X. Wan, Y. Tang, Y. Lv, SiO_2/graphene composite for highly selective adsorption of Pb(II) ion, J. Colloid Interface Sci. 369 (2012) 381–387.
[18] V. Chandra, J. Park, Y. Chun, J.W. Lee, I.-C. Hwang, K.S. Kim, Water-dispersible magnetite-reduced graphene oxide composites for arsenic removal, ACS Nano 4 (2010) 3979–3986.
[19] H.-H. Cho, B.A. Smith, J.D. Wnuk, D.H. Fairbrother, W.P. Ball, Influence of surface oxides on the adsorption of naphthalene onto multiwalled carbon nanotubes, Environ. Sci. Technol. 42 (2008) 2899–2905.
[20] G. Ramesha, A. Vijaya Kumara, H. Muralidhara, S. Sampath, Graphene and graphene oxide as effective adsorbents toward anionic and cationic dyes, J. Colloid Interface Sci. 361 (2011) 270–277.
[21] A. Shafaei, F.Z. Ashtiani, T. Kaghazchi, Equilibrium studies of the sorption of Hg(II) ions onto chitosan, Chem. Eng. J. 133 (2007) 311–316.
[22] S. Verbych, M. Bryk, G. Chornokur, B. Fuhr, Removal of copper(II) from aqueous solutions by chitosan adsorption, Sep. Sci. Technol. 40 (2005) 1749–1759.
[23] J. Rangel-Mendez, R. Monroy-Zepeda, E. Leyva-Ramos, P. Diaz-Flores, K. Shirai, Chitosan selectivity for removing cadmium (II), copper (II), and lead (II) from aqueous phase: pH and organic matter effect, J. Hazard. Mater. 162 (2009) 503–511.
[24] L. Liu, C. Li, C. Bao, Q. Jia, P. Xiao, X. Liu, Q. Zhang, Preparation and characterization of chitosan/graphene oxide composites for the adsorption of Au(III) and Pd (II), Talanta 93 (2012) 350–357.

[25] W.S. Hummers Jr., R.E. Offeman, Preparation of graphitic oxide, J. Am. Chem. Soc. 80 (1958) 1339–1339.
[26] Z. Liu, J.T. Robinson, X. Sun, H. Dai, PEGylated nanographene oxide for delivery of water-insoluble cancer drugs, J. Am. Chem. Soc. 130 (2008) 10876–10877.
[27] G. Zhao, L. Jiang, Y. He, J. Li, H. Dong, X. Wang, W. Hu, Sulfonated graphene for persistent aromatic pollutant management, Adv. Mater. 23 (2011) 3959–3963.
[28] G. Zhao, X. Ren, X. Gao, X. Tan, J. Li, C. Chen, Y. Huang, X. Wang, Removal of Pb(II) ions from aqueous solutions on few-layered graphene oxide nanosheets, Dalton Trans. 40 (2011) 10945–10952.
[29] G. Zhao, J. Li, X. Ren, C. Chen, X. Wang, Few-layered graphene oxide nanosheets as superior sorbents for heavy metal ion pollution management, Environ. Sci. Technol. 45 (2011) 10454–10462.
[30] D. Xu, X. Tan, C. Chen, X. Wang, Removal of Pb(II) from aqueous solution by oxidized multiwalled carbon nanotubes, J. Hazard. Mater. 154 (2008) 407–416.
[31] S.-H. Huang, D.-H. Chen, Rapid removal of heavy metal cations and anions from aqueous solutions by an amino-functionalized magnetic nano-adsorbent, J. Hazard. Mater. 163 (2009) 174–179.
[32] Y. Ho, G. McKay, A comparison of chemisorption kinetic models applied to pollutant removal on various sorbents, Process Saf. Environ. Prot. 76 (1998) 332–340.
[33] Y.-S. Ho, G. McKay, The kinetics of sorption of divalent metal ions onto sphagnum moss peat, Water Res. 34 (2000) 735–742.
[34] R. Han, J. Zhang, W. Zou, J. Shi, H. Liu, Equilibrium biosorption isotherm for lead ion on chaff, J. Hazard. Mater. 125 (2005) 266–271.
[35] X. Xin, Q. Wei, J. Yang, L. Yan, R. Feng, G. Chen, B. Du, H. Li, Highly efficient removal of heavy metal ions by amine-functionalized mesoporous Fe_3O_4 nanoparticles, Chem. Eng. J. 184 (2012) 132–140.
[36] S.J. Allen, P.A. Brown, Isotherm analyses for single component and multi-component metal sorption onto lignite, J. Chem. Technol. Biotechnol. 62 (1995) 17–24.
[37] A.G. Sanchez, E.A. Ayuso, O.J. De Blas, Sorption of heavy metals from industrial waste water by low-cost mineral silicates, Clay Miner. 34 (1999) 469–477.
[38] M. Liu, T. Wen, X. Wu, C. Chen, J. Hu, J. Li, X. Wang, Synthesis of porous Fe_3O_4 hollow microspheres/graphene oxide composite for Cr(VI) removal, Dalton Trans. 42 (2013) 14710–14717.
[39] H.V. Tran, L.D. Tran, T.N. Nguyen, Preparation of chitosan/magnetite composite beads and their application for removal of Pb and Ni(II) from aqueous solution, Mater. Sci. Eng. C. 30 (2010) 304–310.
[40] X. Sun, B. Peng, Y. Ji, J. Chen, D. Li, Chitosan (chitin)/cellulose composite biosorbents prepared using ionic liquid for heavy metal ions adsorption, AIChE J. 55 (2009) 2062–2069.
[41] M.-W. Wan, C.-C. Kan, B.D. Rogel, M.L.P. Dalida, Adsorption of copper (II) and lead (II) ions from aqueous solution on chitosan-coated sand, Carbohydr. Polym. 80 (2010) 891–899.
[42] Y. Liu, Z. Liu, J. Gao, J. Dai, J. Han, Y. Wang, J. Xie, Y. Yan, Selective adsorption behavior of Pb(II) by mesoporous silica SBA-15-supported Pb(II)-imprinted polymer based on surface molecularly imprinting technique, J. Hazard. Mater. 186 (2011) 197–205.
[43] A.R. Kul, H. Koyuncu, Adsorption of Pb(II) ions from aqueous solution by native and activated bentonite: Kinetic, equilibrium and thermodynamic study, J. Hazard. Mater. 179 (2010) 332–339.
[44] D. Ozdes, A. Gundogdu, B. Kemer, C. Duran, H.B. Senturk, M. Soylak, Removal of Pb(II) ions from aqueous solution by a waste mud from copper mine industry: Equilibrium, kinetic and thermodynamic study, J. Hazard. Mater. 166 (2009) 1480–1487.
[45] S.S. Gupta, K.G. Bhattacharyya, Interaction of metal ions with clays: I. A case study with Pb(II), Appl. Clay Sci. 30 (2005) 199–208.
[46] S. Wang, E. Ariyanto, Competitive adsorption of malachite green and Pb ions on natural zeolite, J. Colloid Interface Sci. 314 (2007) 25–31.
[47] R. Shyam, J. Puri, H. Kaur, R. Amutha, A. Kapila, Single and binary adsorption of heavy metals on fly ash samples from aqueous solution, J. Mol. Liq. 178 (2013) 31–36.
[48] Q. Fan, Z. Li, H. Zhao, Z. Jia, J. Xu, W. Wu, Adsorption of Pb(II) on palygorskite from aqueous solution: Effects of pH, ionic strength and temperature, Appl. Clay Sci. 45 (2009) 111–116.